HHS Public Access

Author manuscript

J Mol Biol. Author manuscript; available in PMC 2024 December 01.

Published in final edited form as:

J Mol Biol. 2023 December 01; 435(23): 168317. doi:10.1016/j.jmb.2023.168317.

FDX1 is required for the biogenesis of mitochondrial cytochrome *c* oxidase in mammalian cells

Mohammad Zulkifli[*], **Adriana U. Okonkwo**, **Vishal M. Gohil**[*]

Department of Biochemistry and Biophysics, MS 3474, Texas A&M University, College Station, TX 77843, USA

Abstract

Ferredoxins (FDXs) are evolutionarily conserved iron-sulfur (Fe-S) proteins that function as electron transfer proteins in diverse metabolic pathways. Mammalian mitochondria contain two ferredoxins, FDX1 and FDX2, which share a high degree of structural similarity but exhibit different functionalities. Previous studies have established the unique role of FDX2 in the biogenesis of Fe-S clusters; however, FDX1 seems to have multiple targets in vivo, some of which are only recently emerging. Using CRISPR-Cas9-based loss-of-function studies in rat cardiomyocyte cell line, we demonstrate an essential requirement of FDX1 in mitochondrial respiration and energy production. We attribute reduced mitochondrial respiration to a specific decrease in the abundance and assembly of cytochrome *c* oxidase (CcO), a mitochondrial heme-copper oxidase and the terminal enzyme of the mitochondrial respiratory chain. FDX1 knockout cells have reduced levels of copper and heme a/a_3, factors that are essential for the maturation of the CcO enzyme complex. Copper supplementation failed to rescue CcO biogenesis, but overexpression of heme *a* synthase, COX15, partially rescued COX1 abundance in FDX1 knockouts. This finding links FDX1 function to heme *a* biosynthesis, and places it upstream of COX15 in CcO biogenesis like its ancestral yeast homolog. Taken together, our work has identified FDX1 as a critical CcO biogenesis factor in mammalian cells.

Keywords

Mitochondria; respiration; Copper; Heme *a*; COX1

INTRODUCTION

Ferredoxins (FDXs) are evolutionarily conserved iron-sulfur (Fe–S) cluster containing proteins that act as reducing agents by transferring electrons to multiple target proteins involved in diverse biological processes (1). Mammalian mitochondria contain two FDXs - FDX1 and FDX2 - that share 43% protein sequence identity and are very similar in structure (2). Both FDXs receive electrons from reduced nicotinamide adenine dinucleotide phosphate

[*]Co-corresponding authors: Mohammad Zulkifli, 301 Old Main Drive, MS 3474, Texas A&M University, College Station, TX 77843, USA, mohammad.zulkifli@ag.tamu.edu; Vishal M. Gohil, 301 Old Main Drive, MS 3474, Texas A&M University, College Station, TX 77843, USA, vgohil@tamu.edu.

Author Contributions: M.Z. and V.M.G. designed the research; M.Z and A.U.O performed the research; M.Z and V.M.G. analyzed data and wrote the paper.

(NADPH) via FDX reductase (FDXR) (1). While there is a consensus regarding the source of electrons for FDXs, the identity of in vivo targets of FDX1 has been contentious (3, 5-7). FDX1, also known as adrenodoxin, has been shown to transfer electrons to mitochondrial cytochrome P450 enzymes involved in the metabolism of steroid hormones, bile acids, and vitamins A and D (1, 2). More recently, it was reported that FDX1 donates electrons to kick-start a radical chain reaction in the lipoylation process, a mitochondrial lipid-based post-translational modification seen on two tricarboxylic acid (TCA) cycle enzymes (3, 6). FDX1 has also been implicated in the biogenesis of Fe-S cluster-containing proteins (4, 5), though this aspect of FDX1 function is not supported by recent studies (3, 6). In contrast to the promiscuous nature of FDX1, FDX2 has been shown to specifically donate electrons to the Fe-S biogenesis machinery in mitochondria (2, 4, 5).

Unlike mammalian mitochondria, yeast *Saccharomyces cerevisiae* mitochondria possess only one FDX homolog, the Yeast Adrenodoxin Homolog 1 (Yah1) (1). The protein sequences of FDX1 and FDX2 are approximately 50% identical to Yah1, and like its mammalian homologs, Yah1 receives electrons from the Adrenodoxin Reductase Homolog (Arh1) (7, 8, 9). Thus, Yah1 is expected to possess the functionality of both mammalian ferredoxins. Indeed, Yah1 is involved in the early step of Fe–S biogenesis and lipoylation (3, 7-9). Additionally, Yah1 has also been shown to be required for coenzyme Q (COQ) (10, 11) and heme *a* biosynthesis in yeast (12, 13). Thus, Yah1 is essential for the function and formation of the yeast mitochondrial respiratory chain (MRC) because COQ is a critical lipophilic electron carrier of the MRC (14), and heme *a* is an essential cofactor of cytochrome *c* oxidase (CcO), a copper-heme oxidase that is the terminal enzyme of the MRC (15).

Recently, we reported that FDX1 can catalyze the reduction of copper bound to copper-transporting drugs, thereby releasing it into mitochondria and making it bioavailable to CcO, which contains two copper centers in its active site (16). Additionally, we found that FDX1 can also reduce copper in vitro (16). Together, these findings suggested that FDX1 may also play a role in mitochondrial copper delivery to CcO, prompting us to further investigate the *in vivo* role of FDX1. To this end, we engineered an FDX1 knockout H9c2 rat cardiomyocyte cell line, and a follow-up biochemical, bioenergetics, and genetic characterization of this cell line uncovered a direct role of FDX1 in heme a/a_3 biosynthesis and an indirect role in cellular copper homeostasis. Our findings are consistent with the recently published studies on human FDX1 and previously reported function of the yeast homolog of FDX1 in CcO biogenesis (3, 12).

RESULTS:

Loss of FDX1 results in reduced mitochondrial respiration

To determine the role of FDX1 in mitochondrial bioenergetics, we constructed CRISPR-Cas9-based knockouts of FDX1 in the rat H9c2 cardiac cell line using two different sgRNAs targeting FDX1. FDX1 knockouts were validated in two independent clones ($Fdx1^{-/-}$_1 and $Fdx1^{-/-}$_2) by demonstrating a complete loss of FDX1 protein via SDS-PAGE/immunoblotting (Fig. 1A). To check if FDX1 is required for mitochondrial energy production, we utilized a growth-based nutrient-sensitized assay where wild-type (WT) and

Fdx1$^{-/-}$ cells were grown in glucose or galactose-containing cell culture media. Replacing glucose with galactose forces cells to generate ATP exclusively from glutamine, shifting into a metabolic state where the bulk of cellular energy comes from the mitochondrial oxidative phosphorylation (OXPHOS) (17). In a glucose-containing medium, where a significant fraction of ATP is derived from glycolysis, both WT and *Fdx1*$^{-/-}$ cells showed similar rates of cell proliferation relative to WT cells (Fig. 1B). However, when the cell culture media was switched from glucose to galactose, the *Fdx1*$^{-/-}$ cells showed a severely reduced rate of cell proliferation as compared to WT cells (Fig. 1C). Moreover, the *Fdx1*$^{-/-}$ cells started losing viability in galactose containing media after day 4 (Fig. 1D), suggesting that FDX1 is essential for mitochondrial bioenergetics. To confirm this observation, we measured the oxygen consumption rate (OCR) of these cells and found that *Fdx1*$^{-/-}$ cells showed a pronounced reduction in the basal and maximal OCR (Fig. 1E). Together, these data suggest that FDX1 is essential for mitochondrial respiration and energy production.

FDX1 is required for cytochrome *c* oxidase biogenesis

To unravel the biochemical basis of reduced respiration in *Fdx1*$^{-/-}$ cells, we performed an SDS-PAGE immunoblot analysis of subunits of five OXPHOS complexes. We observed a specific reduction in OXPHOS complex IV (CIV) subunits, COX1 and COX4 (Fig. 2A), suggesting that FDX1 plays a role in the biogenesis of CIV, also known as cytochrome *c* oxidase (CcO) (18). To get a more comprehensive picture of the abundance of fully assembled OXPHOS complexes in *Fdx1*$^{-/-}$ mitochondria, we performed Blue native polyacrylamide gel electrophoresis (BN-PAGE) followed by immunoblot analysis, which revealed that loss of FDX1 did not lead to a defect in the assembly of CI (I and I+III_2), CII, or CIII (III_2 and I+III_2) containing complexes and supercomplexes, however, the higher order CIV-containing supercomplexes were reduced in *Fdx1*$^{-/-}$ cells (Fig. 2B). Probing the membrane with a CIV-specific antibody (COX1), showed a pronounced decrease in the abundance of CIV-containing complexes and supercomplexes (Fig. 2B). Taken together, these results point to a specific role of FDX1 in CcO biogenesis.

Since the abundance of Fe-S-containing subunits of OXPHOS complex II and III, SDHB and UQCRSF1, were unchanged in *Fdx1*$^{-/-}$ cells (Fig. 2A), we questioned the requirement of FDX1 in Fe-S cluster biogenesis. To further probe the role of FDX1 in Fe-S cluster biogenesis, we measured the steady-state levels of mitochondrial aconitase (ACO2) and lipoyl synthase (LIAS), two other Fe-S-containing proteins, and found that their levels were not decreased (Fig. 3A). Next, we checked the functionality Fe-S proteins by measuring mitochondrial aconitase enzyme activity and found it to be decreased by approximately 60% in *Fdx1*$^{-/-}$ cells compared to the WT cells (Fig. 3B). These findings suggest that Fdx1 could indirectly impact the activity of Fe-S proteins.

Loss of FDX1 leads to decreased cellular copper levels

CcO is the only OXPHOS complex that contains copper (Cu) as a cofactor (18). A disruption in Cu delivery to the Cu-containing subunits of CcO, COX1, and COX2 disrupts its assembly and activity, which results in reduced mitochondrial respiration (16). Cu delivery to CcO requires the mobilization of the mitochondrial Cu pool, a process that is not fully understood (18). Based on our recent study showing that FDX1 can reduce Cu(II)

to Cu(I) *in vitro* (16) and our observation that loss of FDX1 results in a specific decrease in CcO (Fig. 2), we reasoned that FDX1 could promote CcO biogenesis by facilitating the mobilization of Cu from the mitochondrial matrix. To directly test the role of FDX1 in cellular Cu homeostasis, we measured cellular and mitochondrial Cu levels in WT and *Fdx1*$^{-/-}$ cells by inductively coupled plasma–mass spectrometry (ICP-MS). We found a specific decrease in intracellular Cu levels in *Fdx1*$^{-/-}$ cells compared to WT cells without any significant changes in iron or zinc levels (Fig. 4A-C). To check how the loss of FDX1 affects mitochondrial metal levels, we quantified the levels of Cu, Fe, and Zn in isolated mitochondria from WT and *Fdx1*$^{-/-}$ cells. Consistent with the reduced cellular Cu levels, we observed a decrease in mitochondrial Cu levels (Fig. 4D). We also noted a small but significant perturbation in mitochondrial Fe and Zn levels that were not apparent in the whole cells (Fig. 4E & F). To independently confirm the decrease in cellular Cu levels, we measured the abundance of the cytosolic Cu metallochaperone for SOD1 (CCS) protein, the levels of which inversely correlate with the cytosolic Cu levels (19). Loss of FDX1 significantly increased the abundance of CCS (Fig. 4G &H). To check if the decrease in Cu levels in *Fdx1*$^{-/-}$ cells is the primary cause of CcO deficiency, we treated *Fdx1*$^{-/-}$ with Cu ionophore Cu-ATSM (diacetylbis(N(4)-methylthiosemicarbazonato) copper (II)), which we have previously shown to rescue Cu deficiency in mammalian cells (16). As expected, Cu-ATSM treatment reduced the abundance of CCS in both WT and *Fdx1*$^{-/-}$ cells (Fig. 4I). However, this treatment did not rescue COX1 levels in *Fdx1*$^{-/-}$ cells (Fig. 4I), suggesting that reduced CcO levels are not due to decreased cellular Cu levels.

FDX1 likely plays a role in heme *a* biosynthesis

In addition to Cu, CcO is also unique in that it is the only OXPHOS complex that contains heme *a*/heme a_3 as essential cofactors (15). The yeast homolog of FDX1, Yah1, has been reported to play a critical role in the formation of heme *a* by heme *a* synthase, Cox15 (12, 13). Based on this information, we reasoned that FDX1 may promote CcO biogenesis by facilitating heme *a* biosynthesis. To check if heme a/a_3 is decreased in *Fdx1*$^{-/-}$ cells, we determined the heme-pyridine redox difference spectra of mitochondrial lysates from WT and *Fdx1*$^{-/-}$ cells. We observed a striking decrease in heme a/a_3 absorption spectra without alteration in heme *b*/*c* in *Fdx1*$^{-/-}$ cells (Fig. 5A). Reduced levels of heme *a* are typically associated with the accumulation of its precursor, heme *o* (20). To test if the accumulated heme *o* can be converted to heme *a*, and rescue COX1 levels, we overexpressed COX15 in *Fdx1*$^{-/-}$ cells and observed a partial rescue of COX1, implicating FDX1 in heme *o* to heme *a* conversion analogous to its yeast counterpart (Fig. 5B-D). Next, we tested if FDX1 or FDX2 have overlapping functions in this process by overexpressing these proteins in *Fdx1*$^{-/-}$ cells and found that FDX1 but not FDX2 can rescue the COX1 and COX4 levels (Fig. 5E & F). To confirm if the rescue in COX1 levels translate to increased CcO activity, we measured OCR in COX15, FDX1, and FDX2 overexpressing *Fdx1*$^{-/-}$ cells. As expected, complementation of *Fdx1*$^{-/-}$ cells with FDX1 completely rescued the OCR to WT levels, suggesting a complete rescue of CcO activity (Fig. 5G). In contrast, FDX2 overexpression did not rescue OCR in *Fdx1*$^{-/-}$ cells (Fig, 5G). Interestingly, COX15 overexpression did not rescue OCR of *Fdx1*$^{-/-}$ cells, suggesting the partial recovery of COX1 protein levels in *Fdx1*$^{-/-}$ cells is not sufficient for restoring CcO activity (Fig. 5B & G). Therefore, we

probed for COX4, another subunit of CcO, in COX15 overexpressing *Fdx1*$^{-/-}$ cells and found that it was not rescued (5H).

DISCUSSION

Cytochrome *c* oxidase (CcO) is a multimeric enzyme that contains Cu and heme groups as essential cofactors that are required for its stability and activity. Biogenesis of a multi-subunit, multi-cofactor containing CcO is an extremely complex process requiring more than 30 assembly factors that are involved in diverse processes, including Cu transport and heme *a*/*a*$_3$ biosynthesis (21, 22). Despite significant progress in our understanding of CcO biogenesis, many gaps in our knowledge still remain. For example, we do not know the biochemical function of many of the known CcO assembly factors, and on a more basic level, it is not clear whether all CcO assembly factors have been identified (21, 22). In this study, we identify FDX1 as a mammalian CcO assembly factor.

Our findings showing reduced oxygen consumption, decreased abundance of CcO, reduced levels of heme *a*/*a*$_3$, and COX15-based partial rescue of COX1 in FDX1 null cells support the role of FDX1 in CcO biogenesis via heme *a*/*a*$_3$ biosynthesis (Figs. 1, 2, and 5). Our results are in line with multiple studies in yeast system. First, in *Schizosaccharomyces pombe*, heme *a* synthase COX15, is fused to YAH1, the yeast gene for mitochondrial ferredoxin, and this fusion protein rescues both *cox15* and *yah1* null mutants of *Saccharomyces cerevisiae* (12). Second, Yah1 was shown to function in conjunction with Cox15 in converting heme o to heme *a*/*a3* (13). Third, rescue of respiratory growth of yeast *yah1* mutant by heterologous expression of human FDX1 and COX15 (3). Additionally, siRNA-based knockdown of FDX1 in human lymphoblast K562 cells has been shown to result in reduced heme levels (5). Despite these evidence, we cannot rule out the possibility that the decrease in heme *a*/*a3* is a consequence rather than a cause for reduced CcO biogenesis in FDX1 null cells. Thus, it is possible that FDX1 promotes CcO biogenesis via yet to be discovered function.

FDX1 deletion led to a mild Cu deficiency in cells (Fig. 4A), which could also contribute to the CcO biogenesis defect because Cu is required for the stability of Cu-containing subunits of CcO (16). However, supplementing cells with Cu ionophore failed to rescue COX1 (Fig. 4I), suggesting that decreased cellular Cu is a consequence of the CcO assembly defect and not a cause. Consistent with this idea, previous studies have shown that CcO assembly defects in human cell lines and mouse tissue trigger a mitochondrial signaling pathway that induces cellular Cu deficiency (23, 24).

Recent studies on FDX1 have uncovered its unexpected role in the biosynthesis of lipoyl cofactor, which is required for the lipoylation of mitochondrial dehydrogenases (3, 6, 25, 26). Whether CcO biogenesis is regulated by lipoylation-related metabolic processes remains to be determined. However, it is well known that lipoylated dehydrogenases of mitochondria, pyruvate dehydrogenase and α-ketoglutarate dehydrogenase, are required for generating reducing equivalents in the form of NADH, which is the primary source of electrons for the mitochondrial respiratory chain. Therefore, the loss of FDX1 could diminish mitochondrial respiration via reduced generation of NADH. In this manner, FDX1

could contribute to mitochondrial respiration via multiple means – NADH generation and CcO biogenesis.

Another possible means by which loss of FDX1 could reduce mitochondrial respiration is via its previously determined role in Fe-S cluster biogenesis (4, 5). This is because many subunits of the OXPHOS complex I, II, and III are Fe-S-containing proteins. Although we did not observe any reduction in the abundance of these Fe-S cluster-containing proteins (Fig. 2), we did observe the reduced activity of ACO2, an Fe-S containing protein of the TCA cycle (Fig. 3). This reduction in ACO2 activity could be due to the known sensitivity of this enzyme to increased oxidative stress, which is expected in mitochondria with increased Fe levels (Fig. 4E). A reduced aconitase activity along with increased mitochondrial Fe content also suggests a possible role of FDX1 in Fe-S cluster biogenesis (5). However, we did not observe any decrease in the steady state levels of Fe-S proteins – results consistent with recently published studies on FDX1 knockout human cell lines (3, 6). In summary, our study has uncovered a yet another function of FDX1, a highly promiscuous mitochondrial reductase, in mammalian CcO biogenesis.

MATERIALS AND METHODS

Mammalian cell culture.

The rat H9c2 cells were cultured in high-glucose Dulbecco's Modified Eagle Medium (DMEM) media supplemented with 10% fetal bovine serum (FBS) (Sigma), 1 mM sodium pyruvate, and Pen/Strep (Life Technologies). Cells were cultured in 5% CO_2 at 37 °C.

Construction of FDX1 knockout and overexpression cell lines.

CRISPR/Cas9-based Fdx1 knockouts were generated as described in (16). For stable overexpression pGenLenti plasmids expressing full-length COX15 (Accession No.: NM_001033699.4), FDX1 (NM_017126.1), and FDX2 (NM_001108002.1), were purchased from GenScript. Lentivirus was generated and transduced in the respective cells as described previously (16). The transduced cells were selected for stable expression of the transgene in the puromycin-containing medium.

Cell proliferation assay.

Cells were seeded at a density of 5 x 10^5 cells/well in 6 well plates. After 16 h, growth media was replaced with fresh growth media containing either high glucose or 10 mM galactose and incubated at 37 °C in 5% CO_2 incubator. Cells were trypsinized and counted at the indicated time points using hemocytometer.

Oxygen consumption rate measurements.

Oxygen consumption rate (OCR) measurements were carried out as previously described (16) with minor modifications. Briefly, cells were seeded in XF24-well cell culture microplates (Agilent Technologies) at 20,000 cells/well in 250 μl of growth media in high glucose DMEM growth media supplemented with 10% FBS and incubated at 37 °C in a 5% CO_2 incubator for ~20 h. Before measurements, 525 μl of the pre-warmed growth medium was added to each well, and cells were further incubated at 37 °C for 30 min in

a non-CO_2 incubator. OCR measurements were carried out in intact cells using Seahorse XF24 extracellular flux analyzer (Agilent Technologies). Mix, wait, and measure timings were set to 2, 2, and 2 min, respectively. For the mitochondrial stress test, oligomycin, carbonyl cyanide 3-cholorophenylhydrazone (CCCP), and antimycin A were sequentially injected to achieve final concentrations of 0.5, 20, and 1 μM, respectively.

Mitochondria isolation.

Mitochondria were isolated using the Mitochondria Isolation Kit from Abcam (ab110170) using the manufacturer's instructions. Protein concentrations were determined by BCA assay (Pierce BCA Protein Assay).

Heme-pyridine redox difference spectra.

The absorption spectra were determined from SDS-solubilized mitochondrial lysates of WT and *Fdx1*$^{-/-}$ according to the method of Berry and Trumpower (27).

SDS-PAGE / BN-PAGE Immunoblotting.

Sodium dodecyl sulfate (SDS)/PAGE and BN-PAGE were performed to separate denatured and native protein complexes, respectively. Cells grown in high glucose DMEM growth media were harvested at 90-95% confluency and washed with phosphate-buffered saline (PBS). For SDS/PAGE sample preparation, whole-cell protein was extracted in RIPA lysis buffer (Boston BioProducts) supplemented with 1x protease inhibitor cocktail (cOmplete Mini EDTA-free; Roche Diagnostics) by incubating cells for 30 min on ice and subsequent centrifugation at 14,000 × g for 15 min at 4°C. Clear supernatants were collected in a fresh tube, and protein concentrations were determined by bicinchoninic acid assay (Pierce BCA Protein Assay). Proteins were separated in 10 or 12% NuPAGE Bis-Tris gel (Thermo Fisher Scientific) followed by transfer onto polyvinylidene fluoride (PVDF) membranes using a Trans-Blot SD semidry transfer cell (Bio-Rad). For BN-PAGE, mitochondria isolated from cells grown in high glucose DMEM growth media were solubilized in a buffer containing 1% digitonin (Thermo Fisher Scientific) at 9 g/g of digitonin to protein ratio, followed by incubation at 4 °C for 15 min and centrifugation at 20,000 × g for 30 min. The clear supernatants were collected, and 1 μl of 50× G-250 sample additive was added. Twenty micrograms of protein were loaded on 3–12% native PAGE Bis-Tris gel (Thermo Fisher Scientific) and transferred to a PVDF membrane using a Mini-PROTEAN Tetra cell (Bio-Rad). Following transfer, the membranes were probed with the following primary antibodies: FDX1, 1:500 (12592-1-AP; Proteintech); NDUFB8, 1:2,500 (ab110242; Abcam); SDHB, 1:1,000 (ab14714; Abcam); UQCRFS1, 1:2,500 (ab14746; Abcam); COX1, 1:1000 (ab14705; Abcam); COX4, 1:2,500 (ab14744; Abcam); ATP5A, 1:2,500 (ab14748; Abcam); CCS, 1:1,000 (sc-55561; Santacruz), and ACTB,1:20,000 (A2228, Sigma). Anti-mouse or anti-rabbit secondary antibodies (1:5,000) were added and incubated for 1 h at room temperature. Blots were developed using Clarity Western ECL or Clarity Max ECL (Bio-Rad Laboratories).

ICP-MS.

Cellular and mitochondrial metal levels were measured by inductively coupled plasma mass spectrometry (ICP-MS) using a Perkin Elmer, NexION 300D instrument. Briefly, cells or mitochondria were harvested and washed with 0.9% NaCl or 300 mM mannitol containing 100 μM EDTA, followed by two more washes to remove EDTA. Cell or mitochondrial pellets were weighed and digested with 40% (w/v) nitric acid (Trace SELECT; Sigma) at 90 °C for 18 h, followed by 4 h digestion with 0.75% H_2O_2 (Sigma Supelco). The samples were then diluted in ultrapure water to 3-5 ml before being injected into the instrument for analysis. Standard curves were generated by serially diluting a premixed standard solution (VWR® ARISTAR® Multi-Element ICP-MS Reference Standards, BDH82026-108) ranging from 1-256 ppb.

RNA isolation and quantitative real-time PCR analysis.

RNA was extracted from a 90% confluent 10 cm dish using the RNeasy mini kit (QIAGEN) according to the manufacturer's instructions. One microgram of total RNA was used as starting material for cDNA synthesis using SuperScript IV VILO Master Mix with ezDNase Enzyme (Thermo Fisher Scientific). Quantitative real-time PCR was performed on CFX96TM Real-Time PCR (Bio-Rad) instrument in a 96-well plate. 20 μl of PCR reactions were prepared with 2× mastermix and 20× Taqman gene expression assay (Cox15: Rn04418844_m1; Fdx2: Rn01486642_g1; Actb: Rn00667869_m1, Thermo Fisher Scientific). The mRNA levels were normalized to Actb expression levels.

Aconitase/citrate synthase activity assay:

Aconitase activity assay was performed using isolated mitochondria as previously described (28) with minor modifications. Briefly, fifty micrograms of dodecylmaltoside solubilized mitochondria were resuspended in 150 μl of aconitase buffer (50 mM Tris-HCl pH 8.0, 50 mM NaCl containing 20 mM isocitric acid) in a clear bottom 96-well plate (Falcon) and increase in absorbance at 235 nm was followed for 10 minutes. The rate of reaction was calculated from the slope of the linear part of the kinetic curve. As controls, activity was also measured in pure buffer or mitochondrial samples resuspended in aconitase buffer without isocitric acid. Citrate synthase activity was measured as previously described (29). Twenty μg of dodecylmaltoside solubilized mitochondria were resuspended in 100 μl of 50 mM Tris-HCl pH 8.0, 50 mM NaCl, and 200 μM of 5,5-dithiobis-(2-nitrobenzoic acid), in a clear bottom 96-well plate (Falcon). Fifty microliters of acetyl-CoA (2 mM) were added to this solution. After 5 min of incubation, the reaction was started by adding 50 μl of oxaloacetate (2 mM), and the turnover of acetyl-CoA was monitored by observing the absorbance at 412 nm for 10 min. The rate of reaction was calculated from the slope of the linear part of the kinetic curve. Aconitase activity was normalized to citrate synthase activity and displayed as a percentage of WT activity.

Statistical analysis and software used:

Statistical analysis was performed using GraphPad Prism 9.4 software using a two-tailed unpaired Student's t-test on data obtained from three or more independent experiments.

GraphPad Prism was also used to generate graphs. ImageJ was used to analyze western blot data, and final figures were prepared using Adobe Illustrator.

ACKNOWLEDGMENTS:

Research reported in this publication was supported by the National Institute of General Medical Sciences of the National Institutes of Health awards R01GM143630 and R01GM111672 and the Welch Foundation Grant A-1810 to VMG. The content is solely the responsibility of the authors and does not necessarily represent the official views of the National Institutes of Health.

Data Availability Statement:

All data are available in the main text.

REFERENCES

1. Schulz V, Freibert SA, Boss L, Mühlenhoff U, Stehling O, Lill R (2023) Mitochondrial [2Fe-2S] ferredoxins: new functions for old dogs. FEBS Lett. 597(1), 102–121. [PubMed: 36443530]
2. Sheftel AD, Stehling O, Pierik AJ, Elsässer HP, Mühlenhoff U, Webert H, Hobler A, Hannemann F, Bernhardt R, Lill R. (2010) Humans possess two mitochondrial ferredoxins, Fdx1 and Fdx2, with distinct roles in steroidogenesis, heme, and Fe/S cluster biosynthesis. Proc. Natl. Acad. Sci. USA 107, 11775–11780. [PubMed: 20547883]
3. Schulz V, Basu S, Freibert SA, Webert H, Boss L, Mühlenhoff U, Pierrel F, Essen LO, Warui DM, Booker SJ, Stehling O, Lill R. (2023) Functional spectrum and specificity of mitochondrial ferredoxins FDX1 and FDX2. Nat. Chem. Biol 19, 206–217. [PubMed: 36280795]
4. Cai K, Tonelli M, Frederick RO, Markley JL. (2017) Human Mitochondrial Ferredoxin 1 (FDX1) and Ferredoxin 2 (FDX2) Both Bind Cysteine Desulfurase and Donate Electrons for Iron-Sulfur Cluster Biosynthesis. Biochemistry 56, 487–499. [PubMed: 28001042]
5. Shi Y, Ghosh M, Kovtunovych G, Crooks DR, Rouault TA. (2012) Both human ferredoxins 1 and 2 and ferredoxin reductase are important for iron-sulfur cluster biogenesis. Biochim. Biophys. Acta 1823, 484–492. [PubMed: 22101253]
6. Dreishpoon MB, Bick NR, Petrova B, Warui DM, Cameron A, Booker SJ, Kanarek N, Golub TR, Tsvetkov P. (2023) FDX1 regulates cellular protein lipoylation through direct binding to LIAS. J. Biol. Chem 13,105046.
7. Lange H, Kaut A, Kispal G, Lill R. A (2000) A mitochondrial ferredoxin is essential for biogenesis of cellular iron-sulfur proteins. Proc. Natl. Acad. Sci. USA 97, 1050–1055. [PubMed: 10655482]
8. Li J, Saxena S, Pain D, Dancis A. (2001) Adrenodoxin reductase homolog (Arh1p) of yeast mitochondria required for iron homeostasis. J. Biol. Chem 276, 1503–1509. [PubMed: 11035018]
9. Mühlenhoff U, Richhardt N, Gerber J, Lill R. (2002) Characterization of iron-sulfur protein assembly in isolated mitochondria. A requirement for ATP, NADH, and reduced iron. J. Biol. Chem 277, 29810–29816. [PubMed: 12065597]
10. Ozeir M, Mühlenhoff U, Webert H, Lill R, Fontecave M, Pierrel F (2011) Coenzyme Q biosynthesis: Coq6 is required for the C5-hydroxylation reaction and substrate analogs rescue Coq6 deficiency. Chem. Biol 18, 1134–1142. [PubMed: 21944752]
11. Pierrel F, Hamelin O, Douki T, Kieffer-Jaquinod S, Mühlenhoff U, Ozeir M, Lill R, Fontecave M. (2010) Involvement of mitochondrial ferredoxin and para-aminobenzoic acid in yeast coenzyme Q biosynthesis. Chem. Biol 17, 449–459. [PubMed: 20534343]
12. Barros MH, Carlson CG, Glerum DM, Tzagoloff A (2001) Involvement of mitochondrial ferredoxin and Cox15p in hydroxylation of heme O. FEBS Lett. 492, 133–138. [PubMed: 11248251]
13. Barros MH, Nobrega FG, & Tzagoloff A. (2002) Mitochondrial ferredoxin is required for heme A synthesis in *Saccharomyces cerevisiae*. J. Biol. Chem 277, 9997–10002. [PubMed: 11788607]

14. Awad AM, Bradley MC, Fernández-Del-Río L, Nag A, Tsui HS, Clarke CF. (2018) Coenzyme Q(10) deficiencies: pathways in yeast and humans. Essays Biochem. 62, 361–376. [PubMed: 29980630]
15. Swenson SA, Moore CM, Marcero JR, Medlock AE, Reddi AR, Khalimonchuk O. (2020) From Synthesis to Utilization: The Ins and Outs of Mitochondrial Heme. Cells 29, 9(3):579. [PubMed: 32121449]
16. Zulkifli M, Spelbring AN, Zhang Y, Soma S, Chen S, Li L, Le T, Shanbhag V, Petris MJ, Chen TY, Ralle M, Barondeau DP, Gohil VM. (2023) FDX1-dependent and independent mechanisms of elesclomol-mediated intracellular copper delivery. Proc. Natl. Acad. Sci. USA 120, e2216722120. [PubMed: 36848556]
17. Gohil VM, Sheth SA, Nilsson R, Wojtovich AP, Lee JH, Perocchi F, Chen W, Clish CB, Ayata C, Brookes PS, Mootha VK. (2010) Nutrient-sensitized screening for drugs that shift energy metabolism from mitochondrial respiration to glycolysis. Nat. Biotechnol 28, 249–255. [PubMed: 20160716]
18. Garza NM, Swaminathan AB, Maremanda KP, Zulkifli M, Gohil VM. (2023) Mitochondrial copper in human genetic disorders. Trends Endocrinol. Metab 34, 21–33. [PubMed: 36435678]
19. Bertinato J & L'Abbé MR (2003) Copper modulates the degradation of copper chaperone for Cu,Zn superoxide dismutase by the 26 S proteosome. J. Biol. Chem 278, 35071–35078. [PubMed: 12832419]
20. Barros MH & Tzagoloff A (2002) Regulation of the heme A biosynthetic pathway in Saccharomyces cerevisiae. FEBS Lett. 516, 119–123. [PubMed: 11959116]
21. Timón-Gómez A, Nývltová E, Abriata LA, Vila AJ, Hosler J, Barrientos A. (2018) Mitochondrial cytochrome c oxidase biogenesis: Recent developments. Semin. Cell Dev. Biol 76, 163–178. [PubMed: 28870773]
22. Barros MH & McStay GP. (2020) Modular biogenesis of mitochondrial respiratory complexes. Mitochondrion 50, 94–114. [PubMed: 31669617]
23. Leary SC, Cobine PA, Kaufman BA, Guercin GH, Mattman A, Palaty J, Lockitch G, Winge DR, Rustin P, Horvath R, Shoubridge EA. (2007) The human cytochrome c oxidase assembly factors SCO1 and SCO2 have regulatory roles in the maintenance of cellular copper homeostasis. Cell Metab. 5(1), 9–20. [PubMed: 17189203]
24. Hlynialuk CJ, Ling B, Baker ZN, Cobine PA, Yu LD, Boulet A, Wai T, Hossain A, El Zawily AM, McFie PJ, Stone SJ, Diaz F, Moraes CT, Viswanathan D, Petris MJ, Leary SC. (2015) The Mitochondrial Metallochaperone SCO1 Is Required to Sustain Expression of the High-Affinity Copper Transporter CTR1 and Preserve Copper Homeostasis. Cell Rep. 10(6), 933–943. [PubMed: 25683716]
25. Tsvetkov P, Coy S, Petrova B, Dreishpoon M, Verma A, Abdusamad M, Rossen J, Joesch-Cohen L, Humeidi R, Spangler RD, Eaton JK, Frenkel E, Kocak M, Corsello SM, Lutsenko S, Kanarek N, Santagata S, Golub TR. (2022) Copper induces cell death by targeting lipoylated TCA cycle proteins. Science 375, 1254–1261. [PubMed: 35298263]
26. Joshi PR, Sadre S, Guo XA, McCoy JG, Mootha VK. (2023) Lipoylation is dependent on the ferredoxin FDX1 and dispensable under hypoxia in human cells. J. Biol. Chem 299(9), 105075. [PubMed: 37481209]
27. Berry EA, & Trumpower BL (1987) Simultaneous determination of hemes a, b, and c from pyridine hemochrome spectra. Anal Biochem 15, 161(1),1–15. [PubMed: 3578775]
28. Pierik AJ, Netz DJ, Lill R. (2009) Analysis of iron-sulfur protein maturation in eukaryotes. Nat. Protoc 4(5), 753–66. [PubMed: 19528951]
29. Zulkifli M, Neff JK, Timbalia SA, Garza NM, Chen Y, Watrous JD, Murgia M, Trivedi PP, Anderson SK, Tomar D, Nilsson R, Madesh M, Jain M, Gohil VM. (2020) Yeast homologs of human MCUR1 regulate mitochondrial proline metabolism. Nat Commun. 11(1), 4866. [PubMed: 32978391]

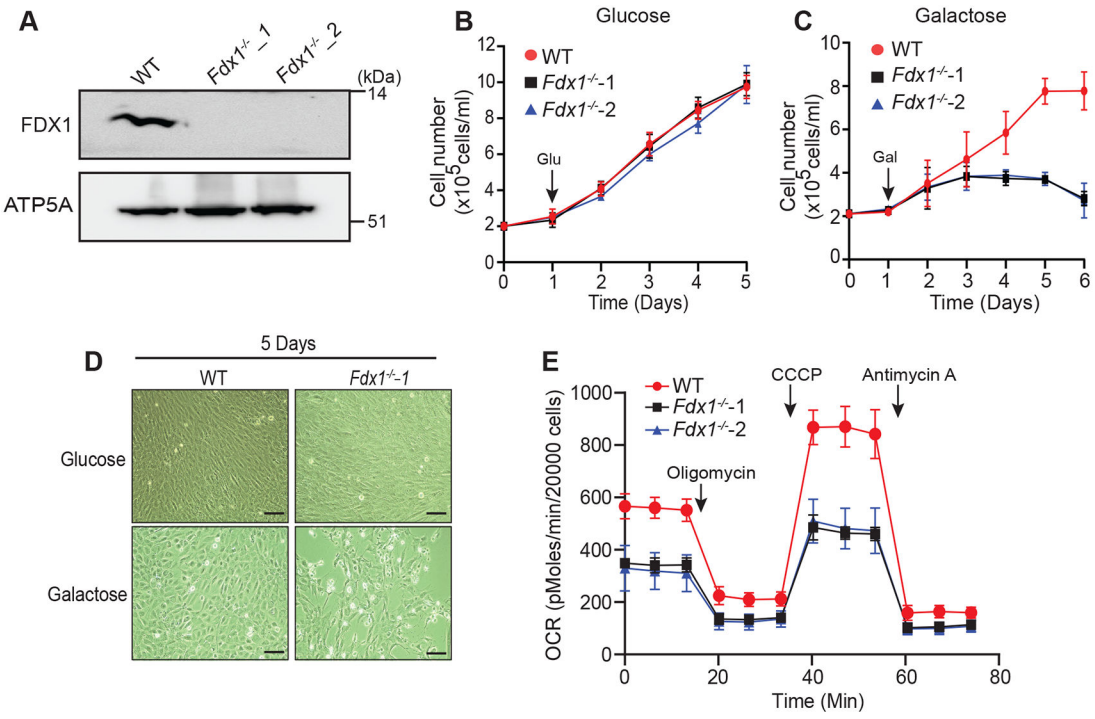

FIGURE 1: FDX1 is required for mitochondrial respiration.

(A) Western blot-based detection of FDX1 in mitochondria isolated from wild-type (WT) cells transduced with either empty vector or sgRNAs targeting Fdx1. *Fdx1*$^{-/-}$-1 and *Fdx1*$^{-/-}$-2 represent two independent clones. ATP5A was used as a loading control. (B & C) Indicated cells were cultured in the high-glucose media in a 6-well plate. After 24 h, the media was replaced with fresh glucose (B) or galactose (C)-containing media (indicated by arrows), and cell numbers were counted and plotted over time. Data are expressed as mean ± SD, n=3. (D) Representative images showing loss of viability in *Fdx1*$^{-/-}$ cells as compared to WT cells in galactose-containing media after 4 days of incubation (n=3) Scale bar:100 μM (E) The oxygen consumption rate (OCR) was measured in WT and *Fdx1*$^{-/-}$ cells in high-glucose media. Oligomycin, CCCP, and antimycin A were used to measure adenosine triphosphate (ATP)-coupled respiration, maximum respiratory capacity, and mitochondria-specific respiration. Data are shown as mean ± SEM, n = 3.

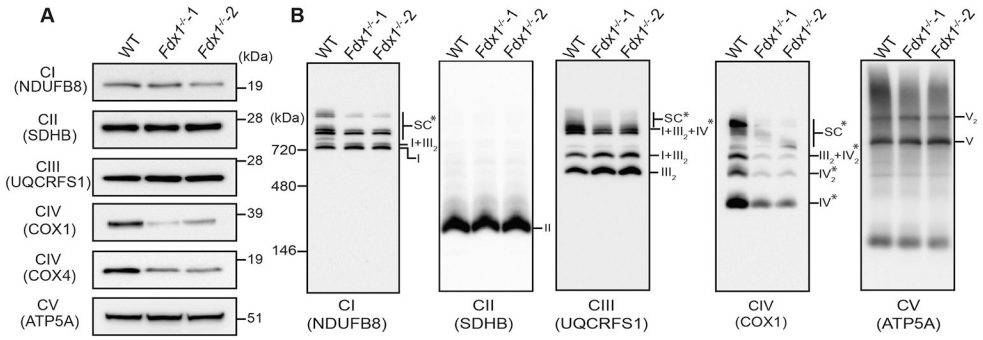

FIGURE 2: Loss of FDX1 decreases cytochrome *c* oxidase abundance.

(A) Cell lysates from WT and *Fdx1*$^{-/-}$ cells grown in high glucose media were analyzed by SDS-PAGE immunoblotting of the indicated subunits of the OXPHOS complexes. (B) BN-PAGE/immunoblot analysis of digitonin-solubilized mitochondria of WT and *Fdx1*$^{-/-}$ cells grown in a high glucose growth medium to detect the abundance of OXPHOS complexes and supercomplexes using the indicated antibodies. The stoichiometry and molecular weights of the complexes and supercomplexes (SC) comprising CI+CIII+CIV are indicated. Data in panels A and B are representative of three independent experiments. *indicates complex IV containing complexes and supercomplexes that are reduced in abundance in *Fdx1*$^{-/-}$ cells.

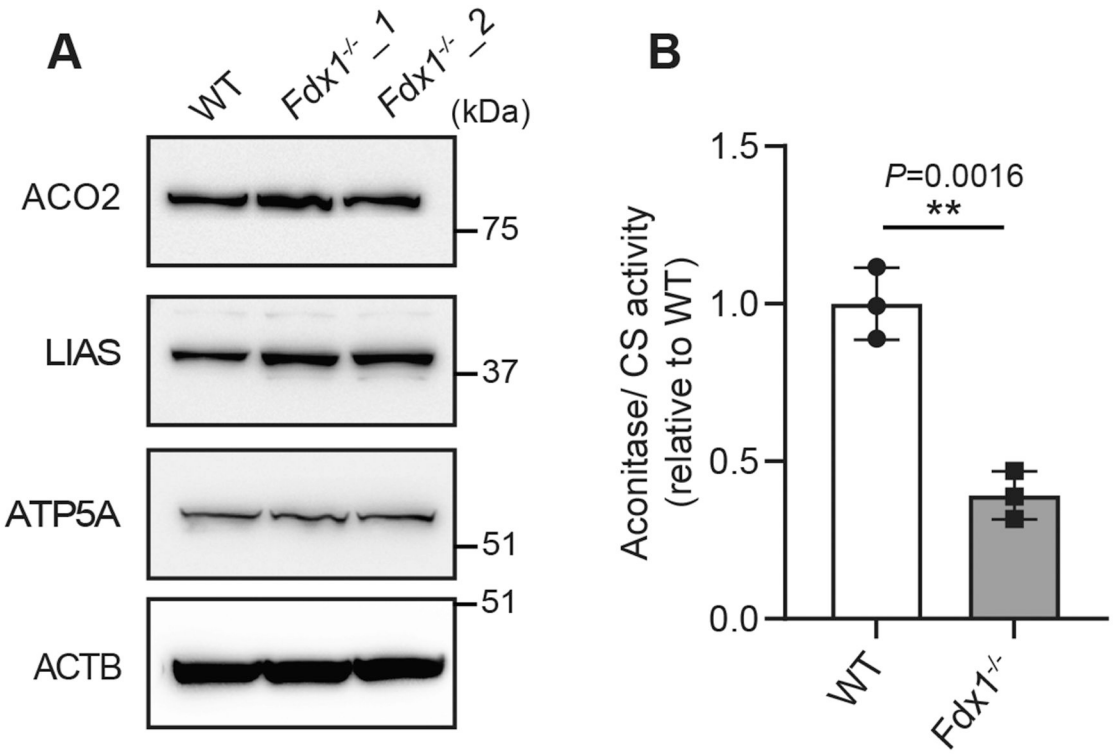

FIGURE 3: Loss of FDX1 results in reduced mitochondrial aconitase activity.

(A) Cell lysates from WT and *Fdx1*$^{-/-}$ were analyzed by SDS-PAGE immunoblotting for ACO2 and LIAS, two mitochondrial Fe-S cluster-containing proteins. ATP5A and ACTB were used as loading controls. (B) Aconitase activity measured in mitochondrial lysates of WT and *Fdx1*$^{-/-}$ cells. The enzymatic activity is normalized to citrate synthase (CS) and expressed relative to WT cells.

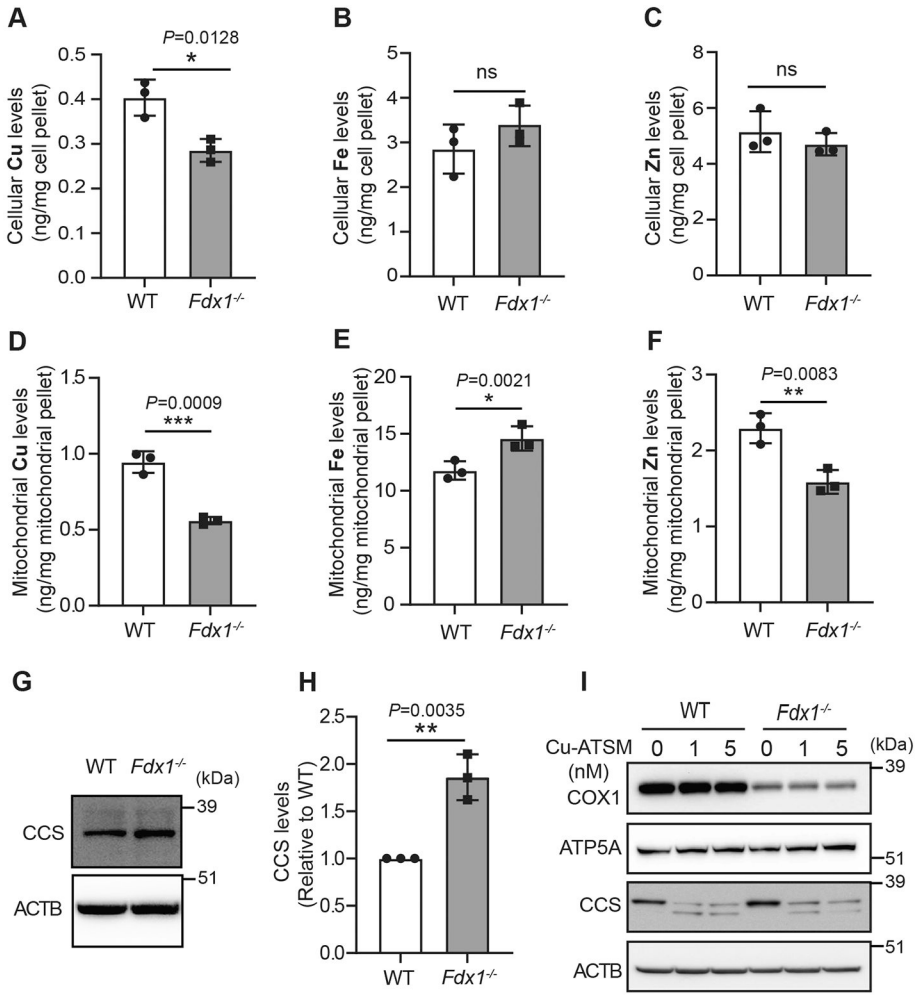

FIGURE 4: Loss of FDX1 leads to cellular copper deficiency and perturbations in mitochondrial metal homeostasis:

(A-F) Cellular and mitochondrial copper (A, D), iron (B, E), and zinc (C, F) content in the WT and *Fdx1*$^{-/-}$ cells were measured by ICP-MS. Data are expressed as mean ± SD; (n = 3). (G) SDS–PAGE/immunoblot analysis of CCS protein levels in WT and *Fdx1*$^{-/-}$ cells. ACTB was used as a loading control. (H) Quantification of CCS levels in panel (G). (I) Immunoblot analysis of COX1 and CCS protein levels in the WT and *Fdx1*$^{-/-}$ cells treated with or without 1 or 5 nM of Cu-ATSM for 48 h. ATP5A and ACTB were used as loading controls.

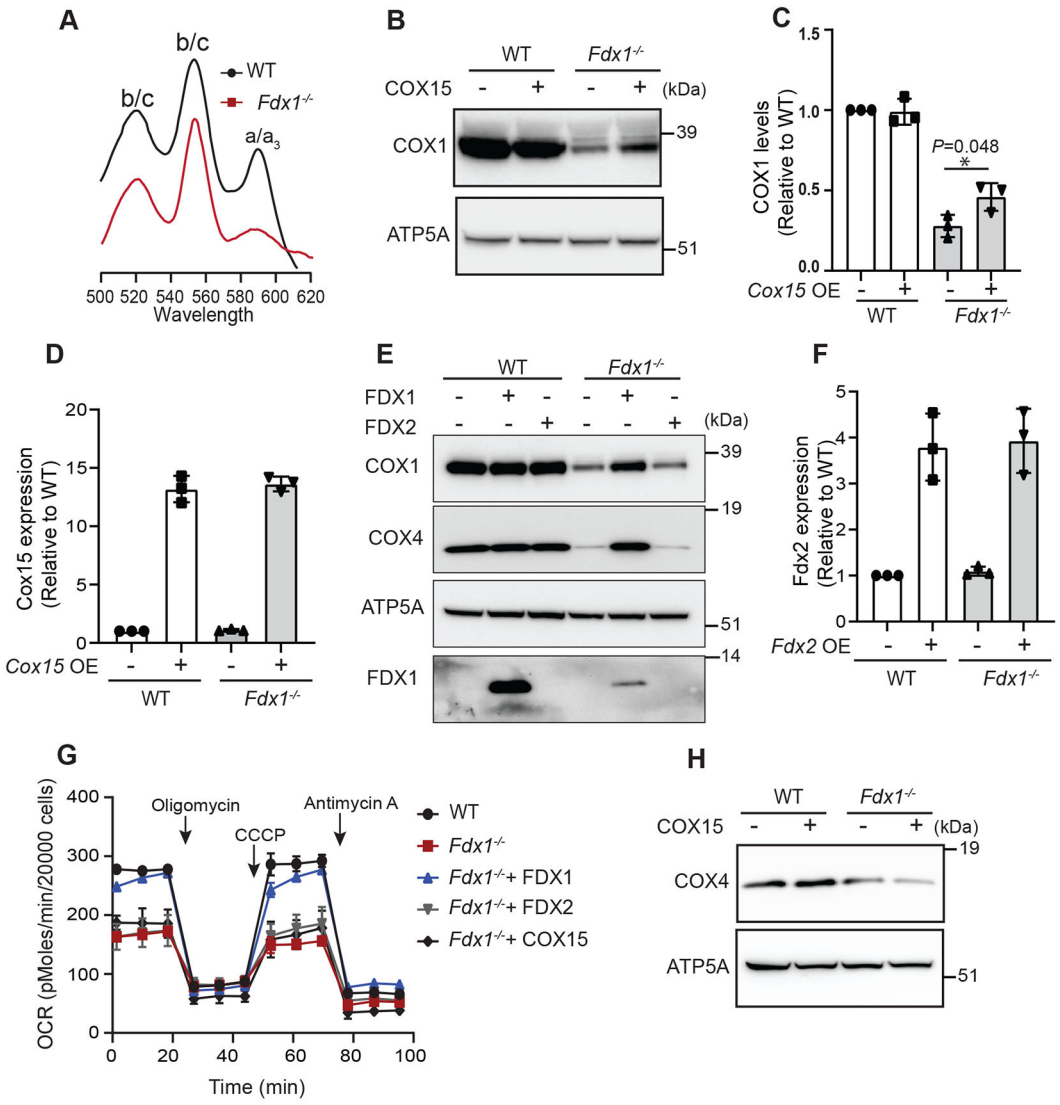

FIGURE 5: FDX1 is required for heme *a* biosynthesis:

(A) Heme-pyridine redox difference spectra of mitochondria from WT and *Fdx1*$^{-/-}$ cells. (B) Immunoblot analysis of COX1 protein levels in the WT and *Fdx1*$^{-/-}$ cells overexpressing COX15. ATP5A was used as a loading control. (C) Quantification of relative COX1 levels in (B), (n = 3). (D) Relative COX15 expression in indicated cells transduced with or without lentivirus harboring COX15 overexpression plasmid. Data are expressed as mean ± SD; (n = 3) (E) Immunoblot analysis of COX1 and COX4 protein levels in the WT and *Fdx1*$^{-/-}$ cells overexpressing FDX1 or FDX2. ATP5A was used as a loading control. (F) FDX2 expression in indicated cells transduced with or without lentivirus harboring FDX2 overexpression plasmid. Data are expressed as mean ± SD; (n = 3). (G) The oxygen consumption rate (OCR) was measured in the indicated cells types in high-glucose media. Oligomycin, CCCP, and antimycin A were used to measure adenosine triphosphate (ATP)-coupled respiration, maximum respiratory capacity, and mitochondria-specific respiration. Data are shown as mean ± SEM, n = 3. (H) Immunoblot analysis of COX4 protein levels

in the WT and *Fdx1*$^{-/-}$ cells overexpressing COX15. ATP5A was used as a loading control. Data in panels A, B, E and H are representative of three independent experiments.